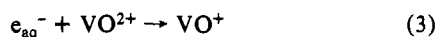


Figure 1. Conductivity signals obtained for the reduction of VO^{2+} by e_{aq}^- at different pHs: squares, experimental results; triangles, calculated signals (see text). Vertical scale: conductivity change, $1 \times 10^{-6} \text{ S cm}^{-1}/\text{division}$.

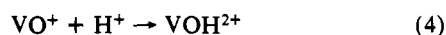
In the presence of such an ion, in our case VO^{2+} , the hydrated electron disappears mainly by



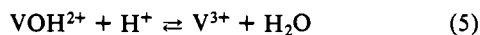
leaving a positive balance of H^+ , which causes a positive residual conductivity signal. The ensuing loss of the "yl" oxygen must be accompanied by the consumption of two protons if V^{3+} is the product. In the pH range studied by us (3.8–4.6), the predominant form of the trivalent vanadium ion is VOH^{2+} (see eq 5 below), so that the loss is reduced to approximately one proton. According to this stoichiometry, the initially positive conductivity signal should decay to nearly zero, and the decay rate would reflect the kinetics of the transition from VO^+ to VOH^{2+} .

Figure 1 shows examples of measured conductivity transients. The signal shapes are as expected, and we observe a decay rate increasing with $[\text{H}^+]$.

With the aid of a kinetic program originally described in ref 11, which was recently modernized and installed on a VAX 11/780 computer, we calculated a model curve for each experiment, based essentially on reaction 3 and

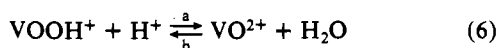


For k_3 , we used our optically measured value of $8 \times 10^{10} \text{ M}^{-1} \text{ s}^{-1}$. k_4 was adjusted to obtain the best fit at all pH values. Our final value was $k_4 = 1.5 \times 10^{10} \text{ M}^{-1} \text{ s}^{-1}$, with an estimated accuracy of $\sim 10\%$. Other parameters needed were taken from the literature: $k_1 = 1.43 \times 10^{11} \text{ M}^{-1} \text{ s}^{-1}$,¹² $k_2 = 2.2 \times 10^{10} \text{ M}^{-1} \text{ s}^{-1}$,¹³ the radiation yield $G(e_{\text{aq}}^-) = 2.8$ particles/100 eV.¹⁴ The equilibrium



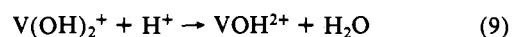
with its $\text{p}K_{\text{a}}$ of 2.26¹⁵ has a slight effect at the lower end of the pH range covered and was therefore included in the calculation.

More difficult was the inclusion of the equilibrium



with a $\text{p}K_{\text{a}}$ of 5.79¹⁵ which significantly altered the kinetics at pH 4.59, and slightly at 4.15. We had to add to our model system

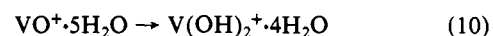
the following postulated reactions (all diffusion-controlled):



We estimated $k_7 = 6 \times 10^{10} \text{ M}^{-1} \text{ s}^{-1}$ (from k_3 , assuming the same diffusion coefficient and reaction radius, but correcting for the different charge of the cation), and by the same procedure, $k_8 = 3.5 \times 10^{10} \text{ M}^{-1} \text{ s}^{-1}$ and $k_9 = 1.5 \times 10^{10} \text{ M}^{-1} \text{ s}^{-1}$ (both from k_4). Calculations showed that all three values were much less critical than the value chosen for k_{6a} . The best fit for pH 4.59 was achieved by using $k_{6a} = 7.5 \times 10^9 \text{ M}^{-1} \text{ s}^{-1}$.

The asymptotic level of the conductivity signals depends somewhat on the difference in ionic equivalent conductance, $\lambda_{\text{VOH}^{2+}} - \lambda_{\text{VO}^{2+}}$. Since no values are known, we adjusted this difference to 10 by using estimated values of $\lambda_{\text{VO}^{2+}} = \lambda_{\text{VO}^+} = 40$ and $\lambda_{\text{VOH}^{2+}} = 50$ (all in $\text{S cm}^2 \text{ equiv}^{-1}$). Other ionic equivalent conductance values were taken from the literature: $\lambda_{\text{H}^+} = 350$, $\lambda_{\text{OH}^-} = 198$, and $\lambda_{e_{\text{aq}}^-} = 185$, with the same units. No other parameter was adjusted. The shape of the electron pulse and the system response time (ca. 50 ns) were also taken into account. The theoretical curves in Figure 1 were calculated by using the entire reaction system described above for all four pH values.

The excellent agreement between the calculated and the measured decay rates and signal amplitudes leads to the conclusion that assumption of a $[\text{H}^+]$ -independent rearrangement reaction such as



is not necessary to interpret the experimental results. The "yl"-type oxygen in the VO^{2+} evidently does not retain its unequal bonding after the one-electron reduction. This is analogous to results of ^{18}O exchange experiments wherein the partial hydrolysis of VO^{2+} causes an internal electronic rearrangement that destroys the unique ($\text{V}=\text{O}$) structure. The marked difference between these results and those previously reported for $\text{Np}(\text{V})$ (i.e., an apparent rate-determining rearrangement step in the reaction scheme) have dictated an attempt to reproduce our original findings.

Registry No. VO^{2+} , 20644-97-7; H_2O , 7732-18-5.

Contribution from the Max-Planck-Institut für Kohlenforschung, D-4330 Mülheim a.d. Ruhr, West Germany

Structure of $[\mu\text{-(CH}_3)_2\text{PCH}_2\text{P(CH}_3)_2]_2\text{Ni}_2(\text{CO})_4$

Klaus R. Pörschke,* Yi-Hung Tsay, and Carl Krüger

Received December 2, 1985

Recently, the reaction of $\text{Ni}(\text{CO})_4$ with the small-bite bidentate ligand bis(dimethylphosphino)methane (abbreviated as dmpm) has been reported in this journal to yield a white precipitate **1**, which was assumed to be $(\text{dmpm})\text{Ni}(\text{CO})_2$ with dmpm as a chelating ligand.¹ Besides two strong terminal infrared $\nu(\text{CO})$ frequencies at 1991 and 1927 cm^{-1} , **1** exhibits in the phosphorus-31 NMR spectrum a single resonance at -15.1 ppm, a surprisingly high-field chemical shift. The authors state that "the volatilities of mononuclear metal carbonyl complexes of $(\text{CH}_3)_2\text{PCH}_2\text{P}(\text{CH}_3)_2$ are generally sufficient for purification by vacuum sublimation and observation of their mass spectra". This contrasts with their

(11) Schmidt, K. H. *Argonne Natl. Lab. [Rep.]*, ANL 1966, ANL-7199; 1970, ANL-7693.

(12) Ertl, G.; Gerischer, H. Z. *Elektrochem.* 1962, 66, 560.

(13) *NBS Handbook* 1973, NSRDS-NBS43.

(14) Michael, B. D.; Hart, E. J.; Schmidt, K. H. *J. Phys. Chem.* 1971, 75, 2798.

(15) Baes, C. F.; Mesmer, R. E. *The Hydrolysis of Cations*; Wiley-Interscience: New York, 1976; p 202.

(1) King, R. B.; Raghuveer, K. S. *Inorg. Chem.* 1984, 23, 2482.

Table I. Summary of Crystal Data and Experimental Details for the Structure Analysis of $[\mu-(\text{CH}_3)_2\text{PCH}_2\text{P}(\text{CH}_3)_2]_2\text{Ni}_2(\text{CO})_4$

Crystal Data	
$a = 10.198$ (1) Å	space group $P2_1/n$
$b = 16.642$ (2) Å	$D_{\text{calc}} = 1.39$ g/cm ³
$c = 14.228$ (1) Å	$\mu = 18.58$ cm ⁻¹
$\beta = 97.68$ (1)°	$T = 20$ °C
$V = 2393$ Å ³	$M_r = 501.7$
$Z = 4$	

Data Measurement
 cryst size: $0.22 \times 0.47 \times 0.58$ mm
 instrument: Enraf-Nonius CAD4
 radiation: Mo $K\alpha$ ($\lambda = 0.71069$ Å), Zr filtered graphite monochromator
 scan mode: coupled $\theta(\text{cryst}) - 2\theta(\text{counter})$
 scan rate: variable $1.0 - 10.0^\circ/\text{min}$
 scan range: $1.0 < \theta < 27.44^\circ$
 scan length: $(0.7 + 0.35 \tan \theta)^\circ$
 no. of reflns measd: 7100 ($\pm h, +k, +l$)

Data Reduction and Structure Solution^a
 abs cor, empirical: max, 1.136; min, 0.814
 no. of indep refltns: 5378
 no. of obsd reflns: 4039 ($I \geq 2\sigma(I)$)
 no. of params: 217
 $R = 0.031$
 $R_w = 0.039$ ($w = 1/\sigma^2(F_o)$)
 goodness of fit: 2.03

^aData reduction: data corrected for background, attenuation, Lorentz, and polarization effects in the usual fashion.⁷ Structure solution: Ni atom positions from a Patterson map; all non-hydrogen atoms located on subsequent Fourier maps; H atoms from difference Fourier maps and as fixed contributions in the final refinement cycles; neutral atomic scattering factors.⁷ Anomalous dispersion: applied to Ni and P atoms.⁷

finding that 1 "sublimes only with extensive decomposition..."¹

On extending our studies on coordination compounds of nickel(0) with $(\text{CH}_3)_2\text{PCH}_2\text{CH}_2\text{P}(\text{CH}_3)_2$ and ethene or ethyne as coligands²⁻⁵ to complexes containing dmpm, we found the binding of bidentate dmpm to nickel(0) in all cases to be bridging rather than chelating.⁶ This prompted us to reexamine the structure of 1.

Large pale yellow plates of 1 may be obtained upon cooling (0 °C) an ethereal solution of equimolar amounts of $\text{Ni}(\text{CO})_4$ and dmpm (10 mmol; 15 mL of ether) after CO evolution has ceased (2 h). No other product was observed on varying the stoichiometry of the reactants. $\nu(\text{CO})$ frequencies and the phosphorus-31 resonance ($\delta -14.0$, $\text{THF}-d_8$) were found to be consistent with those reported. In the 200-MHz proton NMR spectrum ($\text{THF}-d_8$) of 1 a triplet for PCH_2P at $\delta 1.97$ ($^2J(\text{PH}) = 9.1$ Hz) and a pseudotriplet for PCH_3 at $\delta 1.39$ ($\Sigma J(\text{PH}) = 4.2$ Hz) provided no structural information.

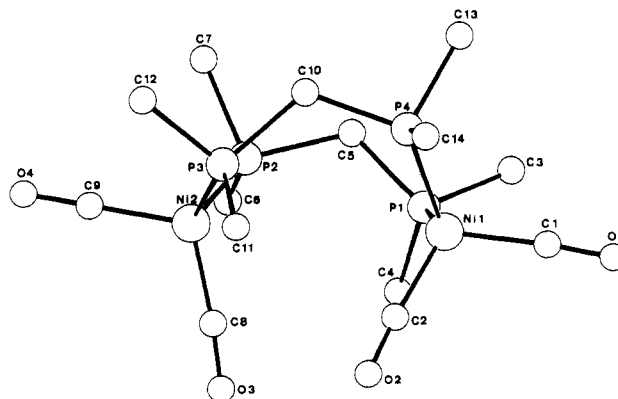
The molecular weight of 1 in benzene was determined by us to be 500 or larger. The mass spectrum (80 °C) showed no molecular peak (expected for dimeric $(\text{dmpm})_2\text{Ni}_2(\text{CO})_4$ at m/e 500), but mass fragments at m/e 472 (1 - CO), 444 (1 - 2 CO), 416 (1 - 3 CO), and 388 ($(\text{dmpm})_2\text{Ni}_2$) were observed, as were also others at m/e 524 and 552, which presumably arise from a thermal rearrangement product of 1. In the 75.5-MHz ¹³C NMR spectrum (δ 200.5 (quintet, CO), 39.0 (heptet, PCH_2P), 22.9 (m, PCH_3); $\text{THF}-d_8$, 40 °C) the multiplets due to spin-spin coupling with phosphorus-31 are deceptively simple and not amenable to

Table II. Final Atomic Coordinates and Their Standard Deviations ($\times 10^4$)

atom	x	y	z
Ni(1)	2338 (1)	696 (1)	3954 (1)
Ni(2)	1793 (1)	3117 (1)	5065 (1)
P(1)	286 (1)	1118 (1)	3563 (1)
P(2)	134 (1)	2998 (1)	3907 (1)
P(3)	3689 (1)	2973 (1)	4479 (1)
P(4)	3646 (1)	1416 (1)	3175 (1)
O(1)	2378 (3)	-979 (2)	3398 (2)
O(2)	3130 (3)	732 (2)	5982 (2)
O(3)	1472 (3)	2130 (2)	6697 (2)
O(4)	1743 (4)	4806 (2)	5574 (3)
C(1)	2380 (3)	-313 (2)	3586 (2)
C(2)	2816 (3)	753 (2)	5187 (2)
C(3)	-650 (4)	526 (3)	2616 (3)
C(4)	-803 (3)	1054 (2)	4496 (3)
C(5)	-51 (3)	2134 (2)	3087 (2)
C(6)	-1519 (3)	3072 (2)	4277 (2)
C(7)	38 (4)	3818 (2)	3052 (2)
C(8)	1623 (3)	2486 (2)	6032 (2)
C(9)	1750 (4)	4142 (2)	5375 (3)
C(10)	3775 (3)	2513 (2)	3307 (2)
C(11)	5041 (3)	2493 (2)	5241 (2)
C(12)	4437 (4)	3946 (2)	4279 (3)
C(13)	3317 (4)	1350 (2)	1880 (2)
C(14)	5378 (3)	1111 (2)	3353 (3)

Table III. Selected Bond Distances (Å) and Angles (deg)

Ni(1)-P(1)	2.207 (1)	P(1)-C(5)	1.836 (3)
Ni(1)-P(4)	2.200 (1)	P(2)-C(5)	1.845 (3)
Ni(2)-P(2)	2.208 (1)	P(3)-C(10)	1.847 (3)
Ni(2)-P(3)	2.219 (1)	P(4)-C(10)	1.840 (3)
P(1)-Ni(1)-P(4)	108.5 (1)	Ni(2)-P(2)-C(6)	114.9 (1)
P(1)-Ni(1)-C(1)	106.7 (1)	Ni(2)-P(2)-C(7)	113.5 (1)
P(1)-Ni(1)-C(2)	111.2 (1)	C(6)-P(2)-C(7)	99.9 (2)
P(4)-Ni(1)-C(1)	109.2 (1)	C(5)-P(2)-C(6)	102.3 (1)
P(4)-Ni(1)-C(2)	111.6 (1)	C(5)-P(2)-C(7)	99.8 (2)
C(1)-Ni(1)-C(2)	109.5 (1)	Ni(2)-P(3)-C(10)	122.2 (1)
P(2)-Ni(2)-P(3)	109.2 (1)	Ni(2)-P(3)-C(11)	116.9 (1)
P(2)-Ni(2)-C(8)	112.6 (1)	Ni(2)-P(3)-C(12)	111.4 (1)
P(2)-Ni(2)-C(9)	103.4 (1)	C(10)-P(3)-C(11)	103.5 (1)
P(3)-Ni(2)-C(8)	114.3 (1)	C(11)-P(3)-C(12)	100.5 (2)
P(3)-Ni(2)-C(9)	104.5 (1)	C(10)-P(3)-C(12)	98.9 (2)
C(8)-Ni(2)-C(9)	111.9 (2)	Ni(1)-P(4)-C(10)	121.9 (1)
Ni(1)-P(1)-C(5)	120.7 (1)	Ni(1)-P(4)-C(13)	115.6 (1)
Ni(1)-P(1)-C(4)	116.2 (1)	Ni(1)-P(4)-C(14)	114.8 (1)
Ni(1)-P(1)-C(3)	113.5 (1)	C(10)-P(4)-C(13)	99.4 (2)
C(3)-P(1)-C(4)	101.2 (2)	C(13)-P(4)-C(14)	99.6 (2)
C(3)-P(1)-C(5)	99.8 (2)	C(10)-P(4)-C(14)	102.0 (1)
C(4)-P(1)-C(5)	102.6 (1)	P(1)-C(5)-P(2)	119.1 (1)
Ni(2)-P(2)-C(6)	123.0 (1)	P(3)-C(10)-P(4)	119.5 (2)

**Figure 1.** Molecular structure of $[\mu-(\text{CH}_3)_2\text{PCH}_2\text{P}(\text{CH}_3)_2]_2\text{Ni}_2(\text{CO})_4$ (1).

detailed analysis, presumably because $J(\text{PP})$ is large. Nevertheless, they are clearly not consistent with a monomeric " $(\text{dmpm})\text{Ni}(\text{CO})_2$ ".

- (2) Pörschke, K. R.; Mynott, R. *Z. Naturforsch., B: Anorg. Chem., Org. Chem.* **1984**, *39B*, 1565.
- (3) Pörschke, K. R.; Mynott, R.; Krüger, C.; Romão, M. J. *Z. Naturforsch., B: Anorg. Chem., Org. Chem.* **1984**, *39B*, 1076.
- (4) Pörschke, K. R.; Mynott, R.; Angermund, K.; Krüger, C. *Z. Naturforsch., B: Anorg. Chem., Org. Chem.* **1985**, *40B*, 199.
- (5) Pörschke, K. R. *Int. Conf. Organomet. Chem.*, *12th* **1985**, 207.
- (6) Pörschke, K. R., to be submitted for publication in *Z. Naturforsch., B: Anorg. Chem., Org. Chem.*

X-ray Structure Determination.⁷ Details of data collection and structure solution are summarized in Table I. Atomic coordinates are listed in Table II, and Table III contains selected bond lengths and angles. A picture of the molecule showing the atomic labeling scheme is presented in Figure 1.

1 exists in the solid state in dimeric units. Two dmpm ligand molecules⁸ serve as bridges between the Ni(CO)₂ groups forming an eight-membered ring. This ring adopts a boat conformation, and the halves of the molecule are related by a pseudo-2-fold axis. The nonbonded Ni-Ni distance is 4.39 Å.

The coordination geometry of the Ni and P atoms may be described as tetrahedral with P-Ni-P angles of 108.5 (1) and 109.2 (1)°. The P-C-P angles of 119.1 (1) and 119.5 (2)° are 10° larger than the ideal tetrahedral angle. The Ni-P bond lengths of 2.200 (1)-2.219 (1) Å are somewhat longer than those observed in (dmpe)(PPh₃)Ni(C₂H₄)³ and (dmpe)Ni(C₂Ph₂)⁴ (2.155-2.179 Å). The average P-C (bridging) distance in **1** (1.842 (5) Å) is comparable to known values.^{3,4} Inspection of intermolecular distances showed no contacts smaller than 3.5 Å (nonhydrogen atoms).

Acknowledgment. We thank Professor O. Stelzer, Wuppertal, for a sample of dmpm and Dr. R. Mynott of this institute for the carbon-13 NMR studies.

Supplementary Material Available: Tables of atomic coordinates and thermal parameters and bond lengths and angles (2 pages). Ordering information is given on any current masthead page. According to policy instituted Jan 1, 1986, the tables of calculated and observed structure factors (17 pages) are being retained in the editorial office for a period of 1 year following the appearance of this work in print. Inquiries for copies of these materials should be directed to the Editor.

- (7) In addition to several locally written programs, the following programs were used: TRACER by Lawton and Jacobson for cell reduction; DATAP by Coppens, Leiserowitz, and Rabinovich for data reduction; DIFABS by Walker and Stuart for empirical absorption correction; Sheldrick's SHELX-76/84 for Fourier calculations and initial least-squares refinement; GFMLS, a highly modified version of ORFLS, by Hirshfeld, Coppens, Leiserowitz, and Rabinovich for subsequent full-matrix least-squares refinement; Davis' DAESD for bond distance and angle calculations; Roberts and Sheldrick's XANADU for best plane and torsion angle calculations; Johnson's ORTEP for the molecular drawings. See: *International Tables for X-ray Crystallography*; Kynoch: Birmingham, England, 1974; Vol. 4.
- (8) For structural data of other dmpm compounds see: (a) Tilley, T. D.; Andersen, R. A.; Zalkin, A. *Inorg. Chem.* **1983**, *22*, 856. (b) Kullberg, M. L.; Kubiak, C. P. *Organometallics* **1984**, *3*, 632. (c) Manojlović-Muir, L.; Ling, S. S. M.; Puddephatt, R. J. *J. Chem. Soc., Dalton Trans.* **1986**, 151.

Contribution from the Department of Chemistry,
Queen's University, Kingston, Ontario, Canada K7L 3N6

Kinetics and Mechanism of the Ligand Substitution Reactions of Pentacyano(ligand)ruthenate(II) Complexes

J. Mark A. Hoddenbagh and Donal H. Macartney*

Received November 13, 1985

The ligand substitution reactions of pentacyanoferrate(II) complexes, Fe(CN)₅L⁽³⁻ⁿ⁾⁻, have been the subject of considerable interest for a number of years.¹⁻⁸ An extensive series of complexes,

Table I. Rate and Activation Parameters for Ligand Substitution of Lⁿ⁺ by Y^{m+} in Ru(CN)₅L⁽³⁻ⁿ⁾⁻ Complexes (pH 7.0, I = 0.10 M)

L ⁿ⁺	Y ^{m+}	10 ⁵ k _{-L} , s ⁻¹	ΔH [‡] , kcal mol ⁻¹	ΔS [‡] , cal K ⁻¹ mol ⁻¹
N-mepyz ⁺	Me ₂ SO	6.31	24.5 ± 0.5	5 ± 2
	py	5.97		
	im	6.74		
	pyz	5.91		
pyrpyr ⁺	Me ₂ SO	4.17	24.0 ± 0.4	2 ± 1
	py	3.79		
	im	4.32		
bpy	Me ₂ SO	6.79	22.2 ± 0.2	-3 ± 1
	pyz	Me ₂ SO	1.77	22.4 ± 1.7
py	N-mepyz ⁺	1.57		
	Me ₂ SO	3.34	25.6 ± 1.3	7 ± 4
im	N-mepyz ⁺	3.39		
	py	10.7	22.2 ± 0.7	-2 ± 2
isonic ⁻	Me ₂ SO	11.7		
	N-mepyz ⁺	1.67	25.1 ± 0.3	4 ± 1
Me ₂ SO	N-mepyz ⁺	1.33		
	py	0.850	24.4 ± 0.4	-1 ± 1
	pyz	0.812		
		0.774		

substituted with N-, O-, S-, and P-donor ligands Lⁿ⁺, have been synthesized from the labile Fe(CN)₅OH₂³⁻ ion. Kinetic, thermodynamic, and volume of activation³ data from numerous mechanistic studies are consistent with a dissociative mechanism for ligand substitutions in these complexes. Correlations between the spectroscopic properties of the Fe(CN)₅L⁽³⁻ⁿ⁾⁻ complexes and other low-spin d⁶ species such as Ru(NH₃)₅L⁽²⁺ⁿ⁾⁺,¹ and recently Ru(CN)₅L⁽³⁻ⁿ⁾⁻,⁹ have been established. These low-spin iron species also represent models for biological systems and have been used in the investigations of specific binding groups in amino acids⁸ and in redox reactions with metalloproteins.¹⁰

In contrast to the work on the pentacyanoferrate(II) complexes, very little has been reported on the analogous ruthenium(II) system until recently. The replacement of the coordinated water ligand in Ru(CN)₅OH₂³⁻ by other ligands, such as aromatic nitrogen heterocycles, gives rise to an equally extensive series of substituted pentacyanoruthenate(II) complexes.¹¹ We have recently reported the results of a kinetic study of the substitution reactions of the Ru(CN)₅OH₂³⁻ ion,¹² which implicates an ion-pair dissociative mechanism, with a water exchange rate of 10 ± 5 s⁻¹, 1 order of magnitude lower than found for the Fe(CN)₅OH₂³⁻ ion.

In the present paper the results of a kinetic study of the ligand-exchange reactions of substituted pentacyanoruthenate(II) complexes are reported. The rate and activation parameters for the dissociation of Lⁿ⁺, where Lⁿ⁺ is dimethyl sulfoxide or a nitrogen heterocycle, from Ru(CN)₅L⁽³⁻ⁿ⁾⁻ have been determined and are compared with values for the analogous pentacyanoferrate(II) complexes and for other ruthenium(II) complexes.

Experimental Section

Materials. Imidazole, isonicotinic acid, 1-(4-pyridyl)pyridinium chloride hydrochloride, pyrazine (Gold Label), and 4,4'-bipyridine hydrate from Aldrich and dimethyl sulfoxide and pyridine from Fisher were used as received. N-methylpyrazinium iodide was prepared by the methylation of pyrazine by methyl iodide in chloroform.^{11,13} The pentacyanoaquo-ruthenate(II) ion, Ru(CN)₅OH₂³⁻, was prepared from the reaction of the Ru(CN)₆⁴⁻ ion (From K₄Ru(CN)₆·3H₂O, Alfa) with bromine in aqueous solution.¹¹ Solutions of the substituted penta-

- (1) (a) Toma, H. E.; Malin, J. M. *Inorg. Chem.* **1973**, *12*, 1039. (b) *Ibid.* **1973**, *12*, 2080.
 (2) Shepherd, R. E. *J. Am. Chem. Soc.* **1976**, *98*, 3329.
 (3) Sullivan, T. R.; Stranks, D. R.; Burgess, J.; Haines, R. I. *J. Chem. Soc., Dalton Trans.* **1977**, 1460.
 (4) Szecey, A. P.; Miller, S. S.; Haim, A. *Inorg. Chim. Acta* **1978**, *28*, 189.
 (5) Toma, H. E.; Martins, J. M.; Giesbrecht, E. *J. Chem. Soc., Dalton Trans.* **1978**, 1610.
 (6) Macartney, D. H.; McAuley, A. *Inorg. Chem.* **1981**, *20*, 748.

- (7) Macartney, D. H.; McAuley, A. *J. Chem. Soc., Dalton Trans.* **1981**, 1780.
 (8) Toma, H. E.; Batista, A. A.; Gray, H. B. *J. Am. Chem. Soc.* **1982**, *104*, 7509.
 (9) Johnson, C. R.; Shepherd, R. E. *Inorg. Chem.* **1983**, *22*, 2439.
 (10) Toma, H. E.; Batista, A. A. *J. Inorg. Biochem.* **1984**, *20*, 53.
 (11) Johnson, C. R.; Shepherd, R. E. *Inorg. Chem.* **1983**, *22*, 1117.
 (12) Hoddenbagh, J. M. A.; Macartney, D. H. *Inorg. Chem.* **1986**, *25*, 380.
 (13) Bahner, C. T.; Norton, L. L. *J. Am. Chem. Soc.* **1950**, *72*, 2881.